Analysis of Electric Sail Heliocentric Motion under Radial Thrust

Alessandro A. Quarta* and Giovanni Mengali†

University of Pisa, I-56122 Pisa, Italy

Nomenclature

A, B	=	constant of integration
a	=	propulsive acceleration modulus [mm/s^2]
a_c	=	spacecraft characteristic acceleration [mm/s^2]
e	=	eccentricity
F	=	dimensionless total energy
H	=	dimensionless constant of motion
p	=	semilatus rectum [au]
r	=	Sun-spacecraft distance [au] (with $r_\oplus \triangleq 1$ au)
t	=	time [days]
x	=	dimensionless variable
β	=	dimensionless characteristic acceleration
θ	=	angular variable [rad]
$\mu_\odot$	=	Sun's gravitational parameter [au^3/day^2]
ν	=	true anomaly [rad]

Subscripts

0	=	initial, parking orbit

*Associate Professor, a.quarta@ing.unipi.it. Associate Fellow AIAA.
†Professor, g.mengali@ing.unipi.it. Senior Member AIAA.

C	=	center
S	=	saddle
I	=	inflection
max	=	maximum
min	=	minimum

Superscripts

$\cdot$	=	time derivative
$'$	=	derivative w.r.t. θ
$\star$	=	critical
$\sim$	=	approximated

Introduction

The motion of a radially accelerated spacecraft in a spherical gravitational field is a classical problem of orbital mechanics. Starting from the pioneering paper by Tsien [1], in which the propulsive acceleration modulus is constant, a number of papers exists that study this problem from different viewpoints, assuming that the thrust-to-mass ratio is a constant of motion [2–5], or a function of either the distance from the primary [6–8] or of the angular variable [9].

The considerable interest for this kind of problem, especially when the radial thrust counteracts the local gravity, is that it captures the main features of special propellantless propulsion systems, such as a photonic solar sail of conic shape [9–11], or the more recent Electric Solar Wind Sail (E-sail) [12–14], whose thrust direction tends to naturally range along the Sun-spacecraft line. A qualitative analysis of an E-sail subjected to an outward radial thrust is thoroughly discussed in [15] in terms of spacecraft total energy. In that paper the thrust modulus, in accordance with the more recent plasma-dynamic simulations by Janhunen [16], is assumed inversely proportional to the Sun-spacecraft distance. In particular, the analysis in [15] emphasizes the existence of heliocentric periodic trajectories

when the E-sail based spacecraft is equipped with a low-performance propulsion system, i.e. when the thrust-to-weight ratio is sufficiently small.

The contribution of this Note is to analyze the heliocentric trajectory of an E-sail with an outward radial thrust by reducing the problem, by means of a suitable change of variables, to the dynamics of a known equivalent nonlinear oscillator with a single degree of freedom. In this sense, the proposed approach completes the graphical analysis discussed in [15]. An analytical, albeit approximate, expression of the spacecraft heliocentric trajectory is also given in polar form when the motion is periodic. This result is shown to be sufficiently accurate for a preliminary mission analysis and is obtained with a reduced computational time, considerably smaller than what is necessary for a numerical integration of the spacecraft equations of motion.

Mathematical model

Consider the dynamics of a spacecraft that initially covers a closed heliocentric parking orbit of given eccentricity $e_0 < 1$ and semilatus rectum p_0. Assume that the spacecraft primary propulsion system is constituted by an E-sail, which, starting from the initial time $t_0 \triangleq 0$, provides a purely radial (outward) propulsive acceleration of modulus $a = a_c \, (r_\oplus/r)$, where r is the Sun-spacecraft distance (with $r_\oplus \triangleq 1\,\text{au}$) and a_c is the (constant) spacecraft characteristic acceleration. The latter, defined as the maximum propulsive acceleration when $r = r_\oplus$, is a parameter that depends on both the propulsion system performance and the spacecraft mass. For example, assuming a spacecraft total mass of 280 kg, a characteristic acceleration of $0.1\,\text{mm/s}^2$ could be obtained using an E-sail with twelve tethers each one being about 4 km long. On the other hand, a more advanced E-sail with 16 tethers of length 6 km each, could be able to provide a characteristic acceleration of $0.3\,\text{mm/s}^2$ for a spacecraft with a total mass of about 300 kg. In both cases the payload mass is assumed to be 100 km [17] .

The spacecraft heliocentric trajectory belongs to the parking orbit's orbital plane and is

described by the Cauchy's problem [15]

$$\dot{\theta} = \frac{\sqrt{\mu_\odot \, p_0}}{r^2} \quad , \quad \ddot{r} = -\frac{\mu_\odot}{r^2} + \frac{\mu_\odot \, p_0}{r^3} + a_c \left(\frac{r_\oplus}{r}\right) \tag{1}$$

$$\theta(t_0) = 0 \quad , \quad r(t_0) = \frac{p_0}{1 + e_0 \, \cos \nu_0} \quad , \quad \dot{r}(t_0) = \sqrt{\frac{\mu_\odot}{p_0}} \, e_0 \, \sin \nu_0 \tag{2}$$

where $\mu_\odot$ is the Sun's gravitational parameter, θ is the angular variable measured counterclockwise from the Sun-spacecraft direction at time t_0, and $\nu_0 \in [-180, \, 180]$ deg is the initial spacecraft true anomaly along the parking orbit. Note that the previous equations take into account that, in this case, the semilatus rectum of the osculating orbit is a constant of motion.

The equivalent nonlinear oscillator

It is now useful to use θ as the independent variable and make the change of variables

$$x \triangleq 1 - \frac{p_0}{r} \quad \text{with} \quad \dot{r} = \sqrt{\frac{\mu_\odot}{p_0}} \, x' \quad \text{and} \quad \ddot{r} = \frac{\mu_\odot}{p_0^2} \, x'' \, (1 - x)^2 \tag{3}$$

where the prime symbol denotes a derivative taken with respect to θ. Accordingly, the second of Eqs. (1) and the last two of Eqs. (2) are rewritten as

$$x'' + x - \frac{\beta}{1 - x} = 0 \quad , \quad x(0) = -e_0 \, \cos \nu_0 \quad , \quad x'(0) = e_0 \, \sin \nu_0 \tag{4}$$

where β is the (constant) dimensionless spacecraft characteristic acceleration defined as

$$\beta \triangleq \frac{a_c \, r_\oplus \, p_0}{\mu_\odot} \tag{5}$$

In the special case in which $\beta = 0$, the spacecraft motion is Keplerian and Eqs. (4) describe the dynamics of a simple harmonic oscillator with an unitary natural frequency [18] (indeed the heliocentric trajectory coincides with the parking orbit). Note that the formulation based on Eqs. (3) is consistent with the classical Burdet-Ferrándiz regularization [19–21] of the two-body motion. A slightly different version of Eqs. (3) has been used by the Authors to analyze the trajectory of a spacecraft subjected to a radial propulsive acceleration of

constant modulus [3] or to a series of radial and tangential impulses [22].

Taking into account Eqs. (4), the variation of the radial distance with angle θ, i.e. the spacecraft heliocentric trajectory in a polar reference frame, is described by the dynamics of an equivalent single-degree-of-freedom nonlinear oscillator. In particular, according to Nayfeh and Mook [23], the first of Eqs. (4) describes the oscillations of a current-carrying wire in the field of an infinite current-carrying conductor restrained by linear elastic springs, where x is the dimensionless distance between the wire and the conductor. Therefore, the available results for this particular nonlinear oscillator [23–25] can be adapted to analyze the heliocentric motion of an E-sail based spacecraft under an outward radial propulsive acceleration. In this sense, Eqs. (4) are firstly used to find the conditions under which a spacecraft heliocentric bounded motion occurs, and then to get an analytical and accurate approximation of the spacecraft heliocentric bounded trajectory.

Trajectory analysis

The formulation of the spacecraft dynamics by means of Eqs. (4) allows important information about the heliocentric trajectory to be obtained without the need of numerically integrating the equations of motion. The succeeding analysis aims at extending the results discussed in [15] using the potential well concept introduced by Prussing and Coverstone [2]. To that end, note that the first of Eqs. (4) can be reduced to a first order differential equation in the form

$$\frac{(x')^2}{2} + F = H \quad \text{with} \quad F \triangleq \frac{x^2}{2} + \beta \, \ln(1 - x) \tag{6}$$

where H is a constant of motion. The latter, taking into account the initial conditions (2), depends on the triplet $\{\beta, e_0, \nu_0\}$ through the equation

$$H = \frac{e_0^2}{2} + \beta \, \ln(1 + e_0 \, \cos \nu_0) \tag{7}$$

Using the constraint $H \geq F(x)$, it is possible to find the range of dimensionless variable x within which the motion is physically admissible. In particular, the values of x such that $H = F(x)$ (that is, $x' = 0$) correspond to distances at which the radial component of the spacecraft inertial velocity is zero, see the second of Eqs. (3).

In Eq. (6) the term F is a sort of potential energy that includes, in addition to the gravitational potential and the potential related to the radial propulsive acceleration, a part of the kinetic energy due to the circumferential component of the spacecraft velocity. The latter is a function of the actual Sun-spacecraft distance only, being equal to $\sqrt{\mu_\odot\, p_0}/r$, which corresponds, in a dimensionless form, to the difference $(1-x)$, see the first of Eqs. (3). When $\beta = 0$, Eq. (6) coincides with the classical energy equation, which is made dimensionless by dividing each term by $\mu_\odot/p_0$. Accordingly, apart from a constant, it can be thought of as the total dimensionless energy of a spacecraft during its propelled motion around the Sun.

When the parking orbit is circular, the constant H is zero independent of β, whereas in a Keplerian motion H takes a nonnegative value equal to $e_0^2/2$. If $e_0 \in (0, 1)$, for a fixed value of β, the constant H varies between a minimum ($H_{\min}$) and a maximum ($H_{\max}$). These two values are reached when the propulsion system is either switched on at the aphelion or at the perihelion of the parking orbit, viz.

$$H_{\min} = \frac{e_0^2}{2} + \beta\, \ln(1 - e_0) \qquad , \qquad H_{\max} = \frac{e_0^2}{2} + \beta\, \ln(1 + e_0) \tag{8}$$

Note that $H_{\max} \geq 0$, whereas $H_{\min}$ can take negative values depending on e_0 and β. Neglecting the trivial case $\beta = 0$ (Keplerian motion) and assuming $x < 1$, the typical variation of $F = F(x)$ with the parameter β is illustrated by the three cases shown in Fig. 1, in accordance with the results discussed in [23] for the equivalent nonlinear oscillator.

When $\beta > 0.25$, $F = F(x)$ is a monotonically decreasing function. Therefore, no closed trajectories exist in the phase plane (x, x') that correspond to a spacecraft bounded motion. In other terms, once the propulsion system is switched on, the spacecraft tracks an open orbit whose perihelion depends on the value of the initial true anomaly ν_0. In particular, if $\nu_0 \in (0,\, 180)$ deg, see the last of Eqs. (4), the spacecraft goes away from the Sun with a radial velocity which is always positive . The perihelion radius is therefore $r_{\min} \triangleq \min(r) = r(t_0)$. If, instead, $\nu_0 \in (-180,\, 0)$ deg, then $x'(0) < 0$ and the spacecraft tends initially to approach the Sun until the radial velocity component becomes zero (equivalently, until $x' = 0$), then the spacecraft tends to indefinitely go away from the Sun. In this case the value of $x_{\min} \triangleq \min(x)$, which gives the perihelion radius $r_{\min} = p_0/(1 - x_{\min})$, is found by numerically evaluating the

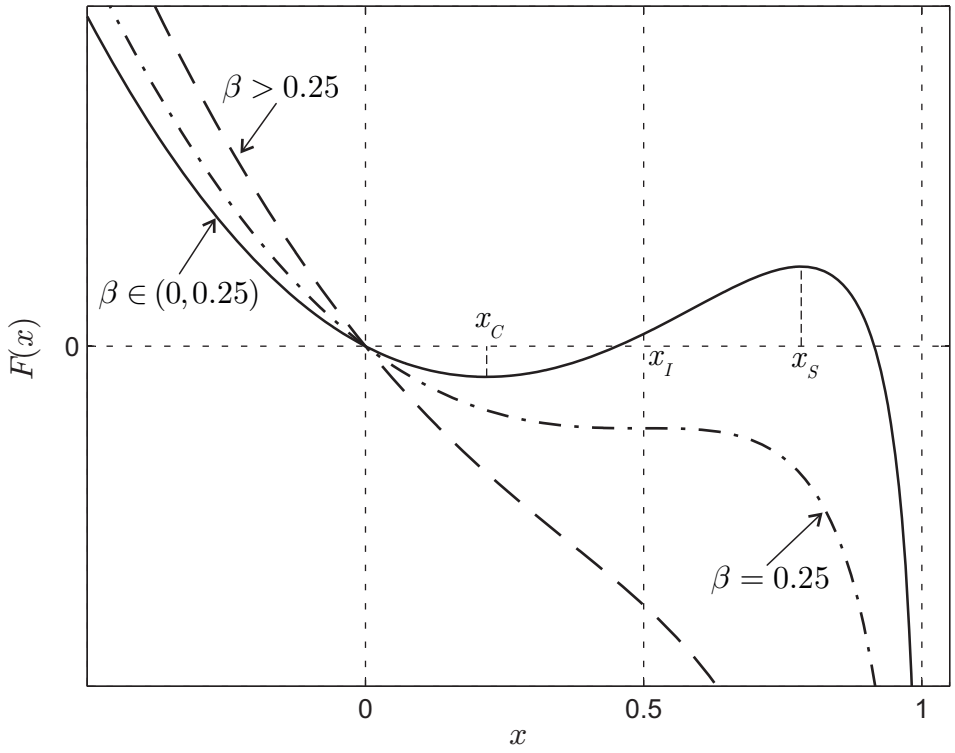

Figure 1: Typical variation of F with x and β, see Eqs. (6).

only real solution of the nonlinear equation $F(x_{\min}) = H$, where H depends on the initial condition through Eq. (7). Finally, when $\nu_0 = \{0, 180\}$ deg, $x'(0) = 0$ and the perihelion radius coincides with the Sun's distance when the propulsion system is switched on, that is $r_{\min} = r(t_0)$. For example, assuming $\beta \equiv e_0 = 0.3$ and an initial true anomaly $\nu_0 = 60$ deg, it is found that $x(0) = -0.15$ and the perihelion radius is $r_{\min} = p_0/1.15$, see Fig 2(a) . Starting instead from the symmetric point with respect to the apse line of the parking orbit, i.e. assuming $\nu_0 = -60$ deg, the result is $H = 0.0869$ and $x_{\min} \simeq -0.226$, which corresponds to a perihelion radius $r_{\min} \simeq p_0/1.226$, see Fig 2(b) .

When $\beta = 0.25$, the function $F = F(x)$ is always decreasing with the exception of a single inflection point of abscissa $x = x_I \triangleq 0.5$, which corresponds to a cusp point [23] in the phase plane (x, x'). The same conclusions discussed for $\beta > 0.25$ can therefore be applied to this case, apart from the point $x(0) = x_I$ and $F(x_I) = H$, which coincides with a closed trajectory, unstable in the sense of Lyapunov. Therefore, recalling Eqs. (6)-(7), the only closed (unstable) orbit for $\beta = 0.25$ is obtained when $e_0 = 0.5$ and $\nu_0 = 180$ deg,

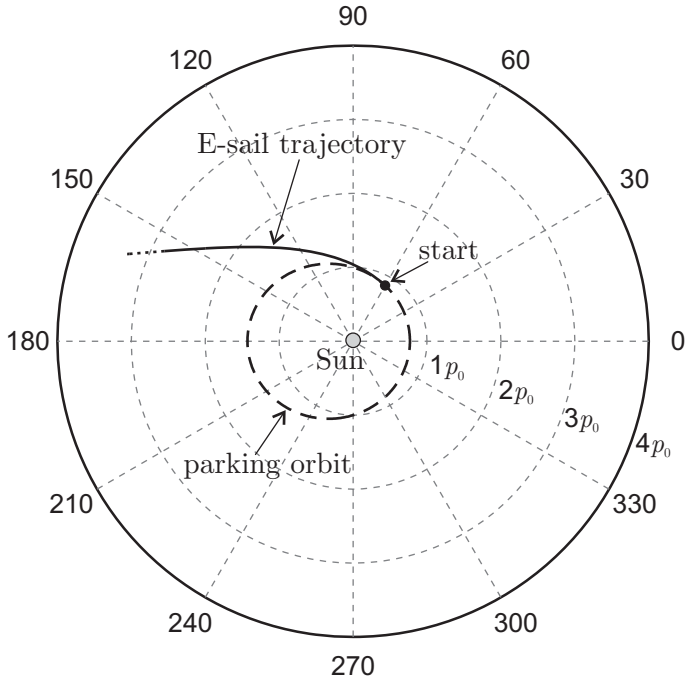

a) $\nu_0 = 60\,\text{deg}$.

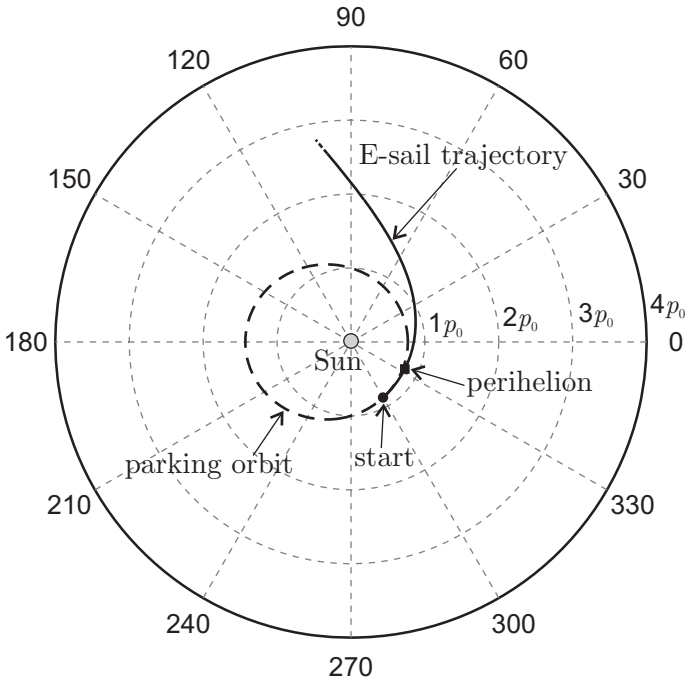

b) $\nu_0 = -60\,\text{deg}$.

Figure 2: E-sail heliocentric trajectory when $\beta = e_0 = 0.3$.

that is, by switching on the propulsion system at the aphelion of the parking orbit when the Sun-spacecraft distance is $2\,p_0$. In that case x does not vary with θ and is always equal to x_I. The corresponding (non-Keplerian) trajectory is therefore circular with radius $r = 2\,p_0$. Other non-Keplerian circular trajectories [15], unstable as well, can be obtained with smaller values of β, as will be discussed next.

A more complex case corresponds to $\beta \in (0,\, 0.25)$, when the function $F = F(x)$ has a local minimum (center) and a local maximum (saddle) [23], at $x = x_C$ and $x = x_S$ respectively, with

$$x_C \triangleq 0.5 - \sqrt{0.25 - \beta} \qquad , \qquad x_S \triangleq 0.5 + \sqrt{0.25 - \beta} \tag{9}$$

The local minimum and maximum points tend to coincide at the inflection point with abscissa x_I when $\beta \to 0.25$, whereas when $\beta \to 0$ the abscissa of the minimum point tends to zero and that of the maximum point tends to unity (therefore r tends to infinity). These two particular values of the dimensionless characteristic acceleration, i.e. $\beta = \{0,\, 0.25\}$, are the bifurcation cases for the motion of the equivalent nonlinear oscillator [23], and imply a qualitative variation of the trajectory in the phase plane which, in its turn, corresponds to a variation in the spacecraft heliocentric trajectory's topology. As a matter of fact, the condition $\beta = 0$ points out the change from a conic orbit to a propelled trajectory. The other case $\beta = 0.25$ represents the change from an open to a (possibly) bounded trajectory, as is now discussed.

For a given pair of initial eccentricity and position along the parking orbit, a bounded trajectory is feasible provided the value of β is such that [23]

$$H \in [F(x_C),\, F(x_S)] \quad \cap \quad x(0) \leq x_S \tag{10}$$

where $F(x_C)$ and $F(x_S)$ are both functions of β only and are obtained by substituting Eqs. (9) into $F = F(x)$, while H is given by Eq. (7). In other terms, a bounded trajectory is possible only if $\beta < \beta^\star \leq 0.25$ where $\beta^\star = \beta^\star(e_0, \cos\nu_0)$, to be found numerically, is the maximum value of β such that the constraints (10) are met. In fact, as long as $\beta < \beta^\star$, the spacecraft tracks a periodic propelled trajectory around the Sun. Figure 3 shows the values

of $\beta^\star$ as a function of the initial orbital eccentricity for different values of the initial true anomaly along the parking orbit.

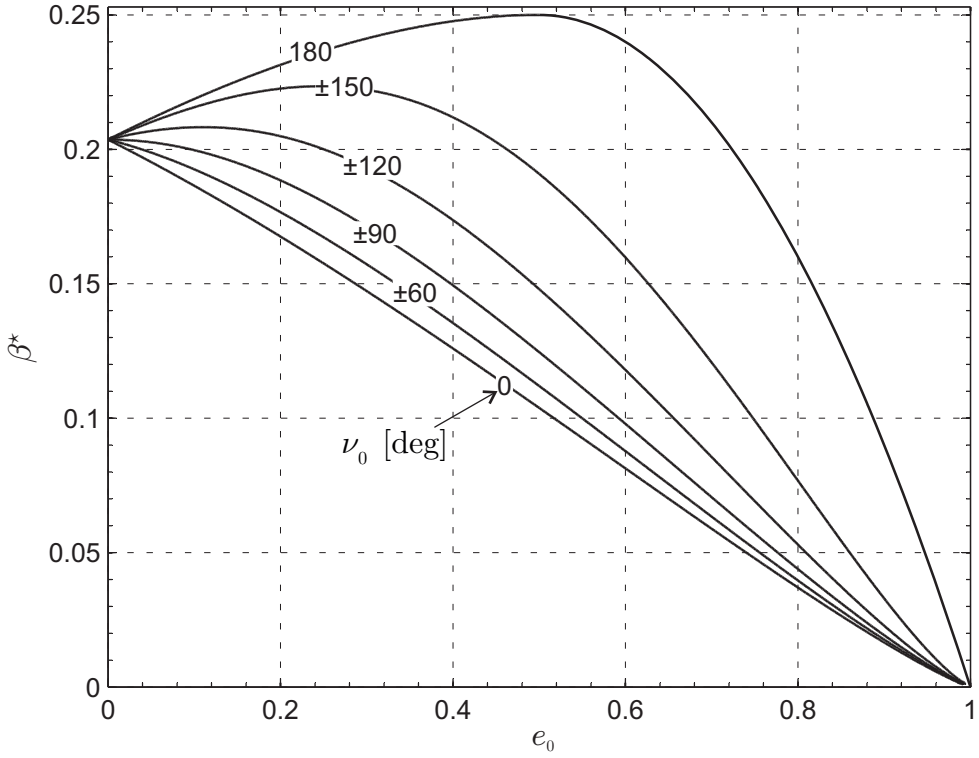

Figure 3: Critical value of dimensionless characteristic acceleration as a function of e_0 and ν_0.

The value of $\beta^\star(e_0, \cos\nu_0)$ is in accordance with the analysis of [15] in which the critical value of β is obtained in graphical form by exploiting the potential well concept. From a mathematical viewpoint, in the critical case of $\beta = \beta^\star$, the level curve in the phase plane (x, x') represents a separatrix [23]. The latter, in terms of spacecraft heliocentric motion, corresponds to a trajectory that asymptotically tends to a non-Keplerian circular orbit [15] with a radius equal to $p_0/(1 - x_S)$. In particular, this non-Keplerian circular orbit, caused by a decreased effective gravitational pull due to the outward radial thrust, is consistent with the so called "shifted circular orbit" discussed in [2] . Note that Fig. 3 provides also the minimum value of the dimensionless characteristic acceleration β required to escape, as a function of the starting true anomaly ν_0. In particular, for a given (elliptic) parking orbit, the absolute minimum of $\beta^\star$ is obtained, as expected [15], starting from the perihelion ($\nu_0 = 0$). Accordingly, the isocontour line corresponding to $\nu_0 = 0$ in Fig. 3 can be found,

for a generic eccentricity e_0, by solving for β the nonlinear equation $H_{\max} = F(x_S)$. Finally note that, as previously stated, the maximum value of $\beta^\star$ consistent with a closed trajectory is $\beta^\star = 0.25$ (see Fig. 3), which is obtained when $e_0 = 0.5$ and $\nu_0 = 180\,\text{deg}$, i.e. when the spacecraft initial position coincides with the orbit's aphelion.

As long as $\beta < \beta^\star$, that is, when the spacecraft trajectory around the Sun is periodic, the aphelion radius $r_{\max}$ and the perihelion radius $r_{\min}$ are obtained by calculating the two roots of equation $F(x) = H$, i.e. $x_{\max}$ and $x_{\min}$ which, from Eq. (2), turn out to be both smaller than x_S. The total angle $\Delta\theta$, swept out by the spacecraft along a single propelled orbit around the Sun, can be calculated by solving Eq. (6) for x' and by separating the variables, to get

$$\Delta\theta = 2 \int_{x_{\min}}^{x_{\max}} \frac{\mathrm{d}x}{\sqrt{2\,H - x^2 - 2\,\beta\,\ln(1-x)}} \tag{11}$$

The value of $\Delta\theta$ is found through a numerical quadrature of Eq.(11). For illustrative purposes, let the initial conditions be $e_0 = 0.3$ and $\nu_0 = 0$, from which $\beta^\star \simeq 0.147$, see Fig. 3. Assuming a dimensionless characteristic acceleration equal to a fifth of the critical value, that is $\beta = 0.03$, it is found that $H \simeq 0.0528$, $x_{\min} = -0.3$ and $x_{\max} \simeq 0.3646$. The corresponding radius of perihelion and aphelion are $r_{\min} = p_0/1.3 \equiv r(t_0)$ and $r_{\max} \simeq p_0/(1 - 0.3646) \simeq 1.574\,p_0$ respectively, as is confirmed by numerical simulations. In this case the anomaly variation necessary to complete a single propelled orbit is, from Eq. (11), equal to $\Delta\theta \simeq 366.5\,\text{deg}$. This implies that the perihelion points of the spacecraft trajectory are all placed along a circle of radius $r(t_0)$ with a relative angular shift of about 6.5 deg. Such an angle also corresponds to the rotation (in the same direction of motion) of the apse line of the osculating orbit during a single revolution, see Fig. 4, which shows the actual E-sail trajectory in a time interval equal to one hundred times the parking orbit's orbital period.

Analytical approximation of bounded trajectories

An important consequence of the reduction of the spacecraft dynamics to an equivalent nonlinear oscillator is that the spacecraft trajectory can be obtained in an approximate analytical form. As a matter of fact, different solutions to the Cauchy's problem of Eq. (4) are available in the literature, either obtained using the Lindstedt-Poincare method [23] or with the harmonic balance method [24].

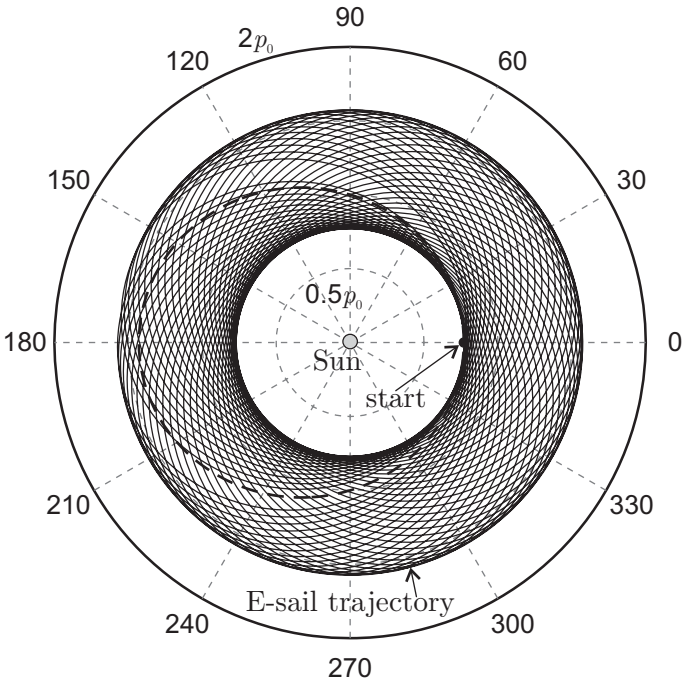

Figure 4: E-sail heliocentric trajectory when $\beta = 0.03$, $e_0 = 0.3$, and $\nu_0 = 0$.

Assuming $\beta < \beta^\star$ and using the procedure described in [23], the approximate solution to the first of Eqs. (4) is

$$x \simeq \widetilde{x} \triangleq x_C + A\cos(\omega\,\theta + B) - \frac{A^2\,\alpha_2}{2\,\alpha_1}\left[1 - \frac{\cos(2\,\omega\,\theta + 2\,B)}{3}\right] \tag{12}$$

where x_C is the center's coordinate and is given by Eq. (9) as a function of β, whereas ω is the approximate value of the frequency of the nonlinear equivalent oscillator, that is

$$\omega = \sqrt{\alpha_1}\left(1 + A^2\,\frac{9\,\alpha_1\,\alpha_3 - 10\,\alpha_2^2}{24\,\alpha_1^2}\right) \tag{13}$$

with

$$\alpha_1 = 1 - \frac{\beta}{(1-x_C)^2} \quad , \quad \alpha_2 = -\frac{\beta}{(1-x_C)^3} \quad , \quad \alpha_3 = -\frac{\beta}{(1-x_C)^4} \tag{14}$$

In Eq. (12) the terms A and B are constant of integration that can be calculated as a function

of the initial conditions, see the last two Eqs. (4), from the following nonlinear equations

$$-e_0 \cos\nu_0 = x_C + A \cos B - \frac{A^2\,\alpha_2}{2\,\alpha_1}\left[1 - \frac{\cos(2B)}{3}\right] \tag{15}$$

$$e_0 \sin\nu_0 = -A\,\omega \sin B - \frac{A^2\,\omega\,\alpha_2}{3\,\alpha_1}\sin(2B) \tag{16}$$

which must be solved numerically. If the propulsion system is switched on either at the perihelion or at the aphelion, that is, if $x'(0) = 0$, the solution of the last two equation is simplified because (16) states that $B = 0$, and (15) can be analytically solved for A. Having calculated the approximate variation of x with θ through Eq. (12), the spacecraft trajectory can be obtained in polar form through the first of Eqs. (3). Note that $\Delta\theta$ can be simply approximated as $2\,\pi/\omega$, which corresponds to the period of the equivalent oscillator.

The effectiveness of approximation given by Eq. (12) can be checked from the previous example in which $\beta = 0.03$, $e_0 = 0.3$ and $\nu_0 = 0$. From Eq. (9) it is found that $x_C \simeq 0.03096$, and from Eqs. (14) $\alpha_1 \simeq 0.968$, $\alpha_2 \simeq -0.0329$, $\alpha_3 \simeq -0.034$. The solution of the nonlinear system (15)-(16) is $A \simeq -0.3322$ and $B = 0$. Accordingly, Eq. (13) provides an estimated frequency $\omega \simeq 0.9824$ and a corresponding swept angle $\Delta\theta \simeq 366.44\,\text{deg}$, which is very close to the actual value of 366.5 deg. This result is by no means surprising as the Lindstedt-Poincare method is well suited [23] for approximating the period of the periodic solutions of Eq. (4) as long as β is far from the critical value $\beta^\star$. In this case the approximate trajectory is nearly coincident with the actual one, obtained by numerically integrating the equations of the oscillator. In fact, it can be checked that the error $|x - \widetilde{x}|$ is always less than one hundredth within twenty full oscillations of the equivalent nonlinear oscillator.

Note that the error is anyway bounded, because the approximate equation (12) is periodic as is the actual solution. A further improvement in the approximation can be obtained from Eq. (13) by using the actual frequency calculated as $\omega = 2\,\pi/\Delta\theta$, where $\Delta\theta$ is given from Eq. (11) via numerical quadrature. When this improved approximation is applied to the previous example, it is found that $\max|x - \widetilde{x}|$ is nearly independent of θ and is always less than 5×10^{-4}. Simulations show that the improved approximation can also be successfully applied to situations in which β is not much smaller than $\beta^\star$. For example, in the previous

case if $\beta = 0.11 \simeq 0.75\,\beta^\star$, the use of the approximate value of ω given by Eq. (13) would imply a maximum position error within twenty orbits of about $0.9\,p_0$, while the same error reduces to $0.04\,p_0$ only using the actual value of ω given by Eq. (11).

Conclusions

The equations of motion of an E-sail based spacecraft with a purely radial thrust have been regularized to reduce the heliocentric trajectory analysis to the dynamics of an equivalent nonlinear oscillator with a single degree of freedom. The advantage of the new approach is that existing mathematical models can be easily adapted to the problem at hand, thus obtaining interesting information on the spacecraft motion (such as the condition under which a bounded motion can take place) as well as an approximate analytical solution to the polar equation of the spacecraft trajectory. The latter result has important practical consequences as it allows the spacecraft position to be successfully estimated, with a reduced computational time, even when the spacecraft performs a number of revolutions around the Sun. The degree of accuracy of the simulations can also be substantially improved by using the actual frequency of the equivalent nonlinear oscillator at the price of introducing an additional numerical quadrature. This technique is well suited for electric sails of low-medium performance. A possible mission scenario could involve the phasing maneuver of an electric sail in a heliocentric orbit. In the latter case, assuming that the parking orbit coincides with that of Earth, the proposed method could be used to calculate the trajectory toward the Sun-Earth triangular Lagrangian points. The trajectory analysis of an E-sail can be extended, with suitable means, to the study of the motion in the presence of a thrust component along the direction orthogonal to the Sun-spacecraft distance. The complication of this scenario is that the semilatus rectum is no longer a constant of motion. Therefore, even in the simplest case of constant thrust angle, it is necessary to calculate how the semilatus rectum of the osculating orbit varies as a function of the spacecraft angular position.

References

[1] Tsien, H. S., "Take-Off from Satellite Orbit," *Journal of the American Rocket Society*, Vol. 23, No. 4, 1953, pp. 233–236.

[2] Prussing, J. E. and Coverstone, V. L., "Constant Radial Thrust Acceleration Redux," *Journal of Guidance, Control, and Dynamics*, Vol. 21, No. 3, May-June 1998, pp. 516–518. doi: 10.2514/2.7609.

[3] Quarta, A. A. and Mengali, G., "New Look to the Constant Radial Acceleration Problem," *Journal of Guidance, Control, and Dynamics*, Vol. 35, No. 3, May-June 2012, pp. 919–929. doi: 10.2514/1.54837.

[4] San-Juan, J. F., López, L. M., and Lara, M., "On Bounded Satellite Motion under Constant Radial Propulsive Acceleration," *Mathematical Problems in Engineering*, Vol. 2012, 2012, pp. 1–12. doi: 10.1155/2012/680394.

[5] Izzo, D. and Biscani, F., "Explicit Solution to the Constant Radial Acceleration Problem," *Journal of Guidance, Control, and Dynamics*, Vol. 38, No. 4, April 2015, pp. 733–739. doi: 10.2514/1.G000116.

[6] Broucke, R., "Notes on the central force r^n," *Astrophysics and Space Science*, Vol. 72, No. 1, September 1980, pp. 33–53. doi: 10.1007/BF00642162.

[7] Boltz, F. W., "Orbital Motion Under Continuous Radial Thrust," *Journal of Guidance, Control, and Dynamics*, Vol. 14, No. 3, May–June 1991, pp. 667–670. doi: 10.2514/3.20690.

[8] Yamakawa, H., "Optimal Radially Accelerated Interplanetary Trajectories," *Journal of Spacecraft and Rockets*, Vol. 43, No. 1, January–February 2006, pp. 116–120. doi: 10.2514/1.13317.

[9] McInnes, C. R., "Orbits in a Generalized Two-Body Problem," *Journal of Guidance, Control, and Dynamics*, Vol. 26, No. 5, September–October 2003, pp. 743–749. doi: 10.2514/2.5129.

[10] Yamakawa, H., "Orbital dynamics of Sun-facing solar sails under the constraint of constant sail temperature," *The Journal of the Astronautical Sciences*, Vol. 54, No. 1, March 2006, pp. 17–27. doi: 10.1007/BF03256474.

[11] Quarta, A. A. and Mengali, G., "Analytical Results for Solar Sail Optimal Missions with Modulated Radial Thrust," *Celestial Mechanics and Dynamical Astronomy*, Vol. 109, No. 2, February 2011, pp. 147–166. doi: 10.1007/s10569-010-9319-x.

[12] Janhunen, P., "Electric Sail for Spacecraft Propulsion," *Journal of Propulsion and Power*, Vol. 20, No. 4, May-June 2004, pp. 763–764. doi: 10.2514/1.8580.

[13] Janhunen, P. and Sandroos, A., "Simulation Study of Solar Wind Push on a Charged Wire: Basis of Solar Wind Electric Sail Propulsion," *Annales Geophysicae*, Vol. 25, No. 3, 2007, pp. 755–767.

[14] Janhunen, P. et al., "Electric solar wind sail: Toward test missions," *Review of Scientific Instruments*, Vol. 81, No. 11, November 2010, pp. 111301–1–111301–11. doi: 10.1063/1.3514548.

[15] Mengali, G., Quarta, A. A., and Aliasi, G., "A Graphical Approach to Electric Sail Mission Design with Radial Thrust," *Acta Astronautica*, Vol. 82, No. 2, February 2013, pp. 197–208. doi: 10.1016/j.actaastro.2012.03.022.

[16] Janhunen, P., "The electric solar wind sail status report," *European Planetary Science Congress 2010*, Vol. 5, Rome, Italy, 19–24 September 2010, Paper EPSC 2010-297.

[17] Janhunen, P., Quarta, A. A., and Mengali, G., "Electric solar wind sail mass budget model," *Geoscientific Instrumentation, Methods and Data Systems*, Vol. 2, No. 1, 2013, pp. 85–95. doi: 10.5194/gi-2-85-2013.

[18] Whittaker, E. T., *A treatise on the analytical dynamics of particles and rigid bodies*, Cambridge University Press, 2nd ed., 1917, pp. 77–93.

[19] Burdet, C. A., "Le mouvement Keplerien et les oscillateurs harmoniques," *Journal für die reine und angewandte Mathematik*, Vol. 1969, No. 238, January 1969, pp. 71–84. doi: 10.1515/crll.1969.238.71.

[20] Ferrándiz, J. M., "A general canonical transformation increasing the number of variables with application to the two-body problem," *Celestial Mechanics and Dynamical Astronomy*, Vol. 41, No. 1–4, March 1987, pp. 343–357. doi: 10.1007/BF01238770.

[21] Fukushima, T., "New Two-Body Regularization," *The Astronomical Journal*, Vol. 133, No. 1, January 2007, pp. 1–10. doi: 10.1086/509606.

[22] Quarta, A. A. and Mengali, G., "Linear Systems Approach to Multiple-Impulse Trajectory Analysis via Regularization," *Journal of Guidance, Control, and Dynamics*, Vol. 33, No. 5, September-October 2010, pp. 1679–1683. doi: 10.2514/1.50133.

[23] Nayfeh, A. H. and Mook, D. T., *Nonlinear Oscillations*, chap. 2, Wiley Classics Library, March 1995, pp. 67–71, ISBN-13: 978-0471121428.

[24] Sun, W. P., Lim, C. W., Wu, B. S., and Wang, C., "Analytical approximate solutions to oscillation of a current-carrying wire in a magnetic field," *Nonlinear Analysis: Real World Applications*, Vol. 10, No. 3, June 2009, pp. 1882–1890. doi: 10.1016/j.nonrwa.2008.02.028.

[25] Ganji, S. S., Barari, A., Fereidoon, A., and Karimpour, S., "On the behaviour of current-carrying wire-conductors and bucking of a column," *Mechanika*, Vol. 19, No. 3, 2013, pp. 306–315. doi: 10.5755/j01.mech.19.3.4659.